BIOCHEMISTRY
including biophysical chemistry & molecular biology

Article

pubs.acs.org/biochemistry

Role of the Occluded Conformation in Bacterial Dihydrofolate Reductases

Enas M. Behiry, Louis Y. P. Luk, Stella M. Matthews, E. Joel Loveridge,* and Rudolf K. Allemann*

School of Chemistry, Cardiff University, Park Place, Cardiff CF10 3AT, United Kingdom

Supporting Information

ABSTRACT: Dihydrofolate reductase (DHFR) from *Escherichia coli* (EcDHFR) adopts two major conformations, closed and occluded, and movement between these two conformations is important for progression through the catalytic cycle. DHFR from the cold-adapted organism *Moritella profunda* (MpDHFR) on the other hand is unable to form the two hydrogen bonds that stabilize the occluded conformation in EcDHFR and so remains in a closed conformation during catalysis. EcDHFR-S148P and MpDHFR-P150S were examined to explore the influence of the occluded conformation on catalysis by DHFR. Destabilization of the occluded conformation did not affect hydride transfer but altered the affinity for the oxidized form of nicotinamide adenine dinucleotide phosphate ($NADP^+$) and changed the rate-determining step of the catalytic cycle for EcDHFR-S148P. Even in the absence of an occluded conformation, MpDHFR follows a kinetic pathway similar to that of EcDHFR with product release being the rate-limiting step in the steady state at pH 7, suggesting that MpDHFR uses a different strategy to modify its affinity for $NADP^+$. DHFRs from many organisms lack a hydrogen bond donor in the appropriate position and hence most likely do not form an occluded conformation. The link between conformational cycling between closed and occluded forms and progression through the catalytic cycle is specific to EcDHFR and not a general characteristic of prokaryotic DHFR catalysis.

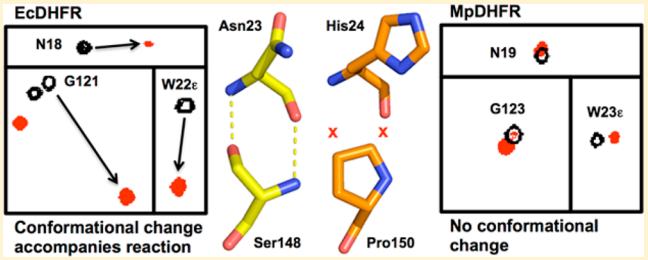

Dihydrofolate reductase (DHFR) catalyzes the reduction of 7,8-dihydrofolate (DHF) to 5,6,7,8-tetrahydrofolate (THF) in the presence of reduced nicotinamide adenine dinucleotide phosphate (NADPH). DHFR is important for maintaining the intracellular pool of THF, a cofactor involved in many biological reactions that require transfer of a one-carbon unit, such as biosynthesis of thymidylate, purines, and some amino acids. Hence, DHFR is a major target for anticancer and antibacterial drugs.[1]

During catalysis, DHFR from *Escherichia coli* (EcDHFR) cycles through five intermediates, E·NADPH, E·NADPH·DHF, E·$NADP^+$·THF, E·THF, and E·NADPH·THF, with product release from the mixed ternary complex E·NADPH·THF being the rate-limiting step at pH ≤7 under steady state conditions (Figure S1, Supporting Information).[2] The M20 loop (residues 9−24) of EcDHFR switches between two conformations during the catalytic cycle (Figure 1A). In reactant complexes E·NADPH and E·NADPH·DHF, this loop adopts the "closed" conformation, packing against NADPH and preventing access of the solvent to the active site. This conformation is stabilized by hydrogen bonds between residues in the M20 loop and the FG loop (residues 116−132), namely, Gly15(O) to Asp122(HN) and Glu17(HN) to Asp122(Oδ2) (Figure 1B).[2,3] In the product binary and ternary complexes, on the other hand, the M20 loop switches to the "occluded" conformation (Figure 1C). The two hydrogen bonds between the M20 loop and FG loop that stabilize the closed conformation are disrupted, and the occluded conformation is instead stabilized by two hydrogen bonds between Asn23 (O and HN) in the M20 loop and Ser148 (HN and Oγ) in the GH loop (residues 142−149) (Figure 1C).[2] The nicotinamide group of the cofactor is blocked from entering the active site by the M20 loop and protrudes into solution. It has been proposed that movement between the closed and occluded conformations is important for both modifying ligand affinity and aiding progression through the catalytic cycle.[2,4]

Previous work on DHFR from *Moritella profunda* (MpDHFR), a cold-adapted bacterium isolated from deep-sea sediments,[5] investigated the effect of temperature and pressure on the structure and thermodynamic stability as well as the steady state and pre-steady state kinetics of the enzyme.[6−10] Although MpDHFR and EcDHFR have very similar crystal structures[8] and the two enzymes have 55% identical sequences,[6] Ser148 of EcDHFR is replaced with proline in MpDHFR, which therefore cannot form either of the hydrogen bonds that stabilize the occluded conformation. Indeed, the occluded conformation has not been observed in other bacterial DHFRs, including complexes of DHFRs from *Lactobacillus casei* (LcDHFR)[11,12] and *Bacillus anthracis* (BaDHFR)[13] that form the occluded conformation in EcDHFR. BaDHFR has a proline residue at position 148 (EcDHFR numbering), while in LcDHFR,[11] Ser148 is replaced with alanine. Alanine can in principle form

Received: April 27, 2014
Revised: July 10, 2014
Published: July 11, 2014

   dx.doi.org/10.1021/bi500507v | *Biochemistry* 2014, 53, 4761−4768

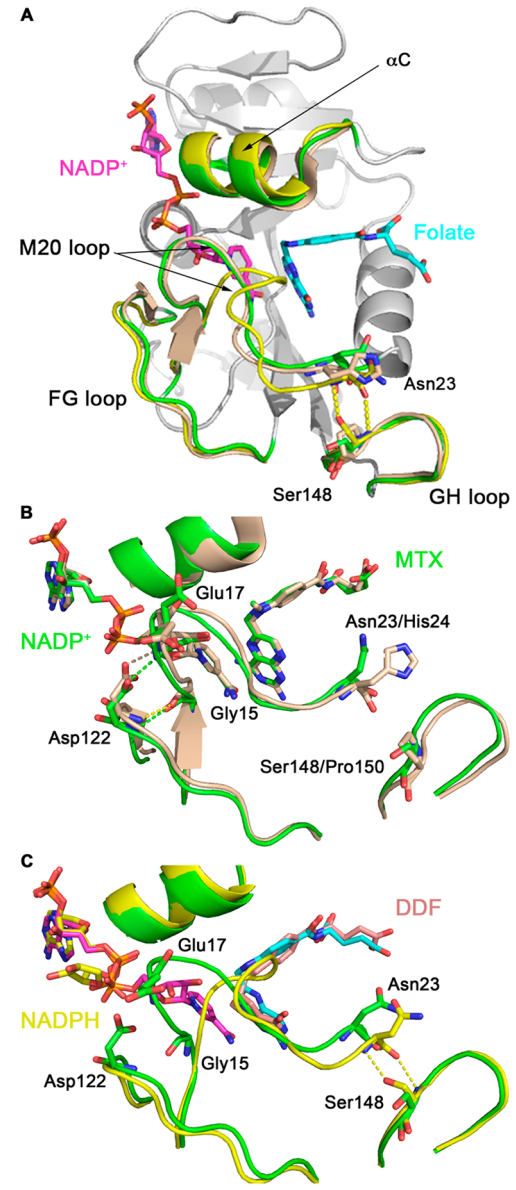

Figure 1. (A) Cartoon representation of EcDHFR (gray, PDB entry 1RX2)[1] in the closed conformation. Important structural elements are colored green. Positions of the M20, FG, and GH loops are shown in the occluded conformation in EcDHFR (yellow, PDB entry 1RX6)[2] and in the closed conformation in MpDHFR (wheat, PDB entry 3IA4).[8] Ligands are shown as sticks; folate is colored cyan and $NADP^+$ pink. (B) Alignment of the active site loops of EcDHFR (green, PDB entry 1DRE)[2] and MpDHFR (wheat, PDB entry 3IA4)[8] in complex with methotrexate (MTX) and NADPH showing residues forming hydrogen bonds that stabilize the closed and occluded conformations in EcDHFR, and corresponding residues in MpDHFR. Hydrogen bonds stabilizing the closed conformations are shown as dashed lines. (C) Alignment of the active site loops of EcDHFR in the closed conformation (green, PDB entry 1RX2)[2] with ligands as described for panel A and in the occluded conformation (yellow, PDB entry 1RX6)[2] with 5,10-dideazatetrahydrofolate (DDF) in pale pink and NADPH in yellow, showing residues forming hydrogen bonds that stabilize the closed and occluded conformations. Hydrogen bonds stabilizing the occluded conformation are shown as dashed yellow lines.

the backbone hydrogen bond with Asn23 but not the side chain hydrogen bond (Figure S2, Supporting Information), although EcDHFR-S148A is known to adopt the closed conformation in the product complex rather than an occluded conformation.[14] Despite its inability to form the occluded conformation, LcDHFR is known to have a catalytic cycle very similar to that of EcDHFR.[15] In addition to MpDHFR, BaDHFR, and LcDHFR, DHFRs from a number of other organisms have an alternative residue in place of Ser148 (Figure S3, Supporting Information). It is unlikely that these DHFRs are able to form the occluded conformation, and it is therefore of interest to investigate the importance of the occluded conformation in DHFR catalysis.

To this end, EcDHFR-S148P and MpDHFR-P150S were generated. Our results confirm that the occluded conformation assists the release of the oxidized cofactor $NADP^+$ and progression through the catalytic cycle but suggest that alternative strategies are adopted by those bacterial DHFRs incapable of forming this conformation.

MATERIALS AND METHODS

Chemicals. $NADP^+$ and NADPH were purchased from Melford. Folate was purchased from Sigma. Dihydrofolate was prepared by dithionite reduction of folate.[16] Tetrahydrofolate was synthesized enzymatically from dihydrofolate using EcDHFR[17] in the presence of alcohol dehydrogenase from *Thermoanaerobacter brockii*, 2-propanol, and $NADP^+$ and purified using a Dionex ICS3000 fast protein liquid chromatograph. 4-(*R*)-NADPD was prepared as described previously.[18] All DHFRs were produced as reported previously[9] and purified by anion exchange chromatography on Q-Sepharose resin followed by size exclusion chromatography on a Superdex 75 column. The concentrations of NADPH/NADPD, $NADP^+$, and MTX were determined spectrophotometrically using extinction coefficients of 6200 cm^{-1} M^{-1} at 339 nm,[19] 18700 cm^{-1} M^{-1} at 260 nm,[20] and 22100 cm^{-1} M^{-1} at 302 nm,[21] respectively. An extinction coefficient of 28000 cm^{-1} M^{-1} was used to determine the concentrations of DHF and THF at 282 and 297 nm, respectively.[22,23]

Site-Directed Mutagenesis. The Finnzymes Phusion site-directed mutagenesis kit and the following primers were used to generate MpDHFR-P150S and EcDHFR-S148P: MpDHFR-P150S, 5′-GCGGCAGATGATAAAAACTCGCATAATTAC-CGC-3′; and EcDHFR-S148P, 5′-GCTGATGCGCAGAACC-CTCACAGCTATTGC-3′. Replaced bases are underlined.

Circular Dichroism Spectroscopy. An Applied Photophysics Chirascan spectrophotometer was used to measure spectra between 195 and 400 nm using 10 μM protein in 5 mM potassium phosphate (pH 7.0) in a quartz cuvette (0.1 cm path length, Helma) under N_2. Mean residue ellipticities ($[\Theta]_{MRE}$) were calculated using the equation $[\Theta]_{MRE} = \Theta/(10ncl)$, where Θ is the measured ellipticity in millidegrees, n is the number of backbone amide bonds, c is the concentration of protein in moles per liter, and l is the path length in centimeters. Melting temperatures were determined by plotting $[\Theta]_{MRE}$ at 222 nm against temperature.

Nuclear Magnetic Resonance (NMR) Experiments. All NMR experiments were performed on a Bruker AVANCE III 600 MHz spectrometer with a QCI-P cryoprobe at 20 °C in 50 mM Tris-HCl buffer (pH 7.0) containing 1 mM NaCl and 10 mM β-mercaptoethanol. A 10-fold excess of ligands was used. An equimolar solution of both ligands ($NADP^+$ and folate or $NADP^+$ and THF) was prepared and adjusted to pH 7.0 before addition to the DHFR; the pH was then checked before measurement of the spectrum. D_2O (5%) was added to all the NMR samples before spectra were acquired. Spectra were

dx.doi.org/10.1021/bi500507v | *Biochemistry* 2014, 53, 4761−4768

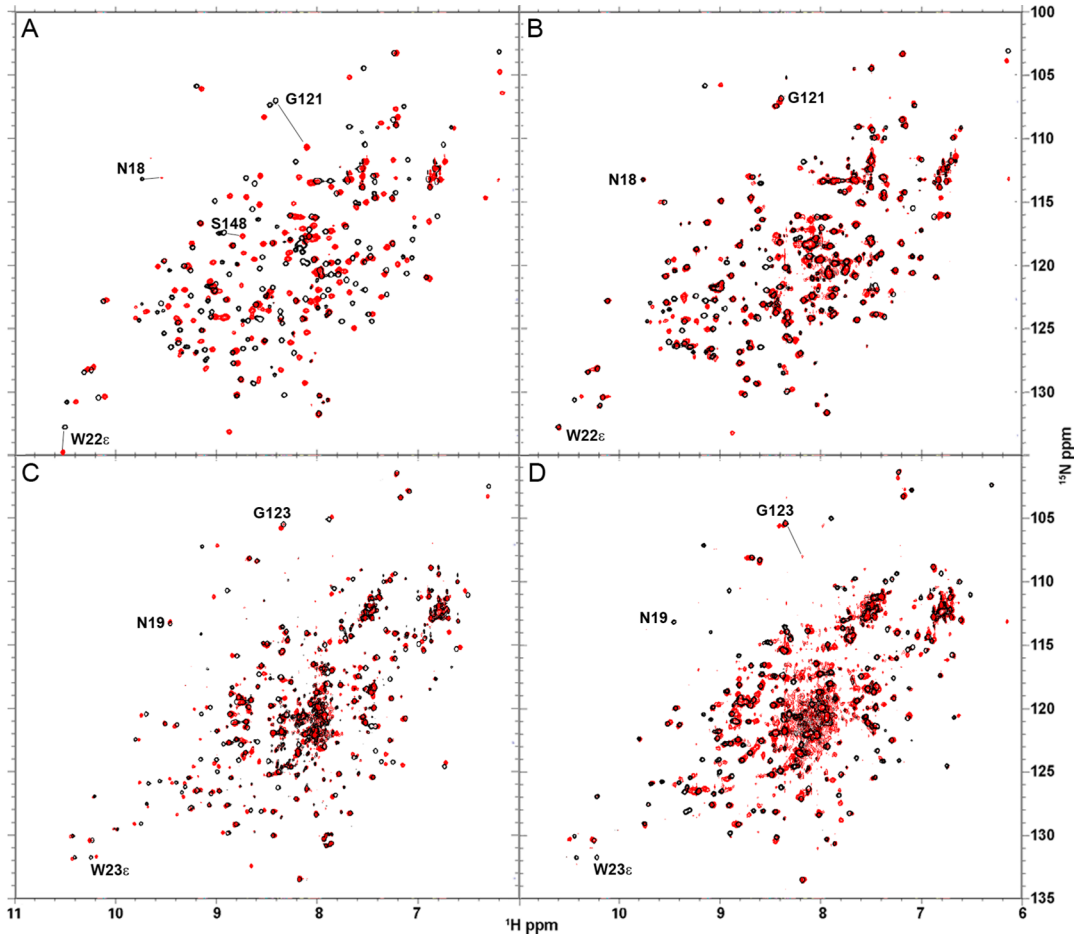

Figure 2. $^{1}H-^{15}N$ HSQC spectra of the DHFR·NADP^{+}·folate (black) and DHFR·NADP^{+}·THF (red) complexes of (A) EcDHFR, (B) EcDHFR-S148P, (C) MpDHFR, and (D) MpDHFR-P150S at 25 °C. Residues showing large amide chemical shift changes between the closed and occluded conformations in EcDHFR are indicated (A). It can be seen that these residues do not display large chemical shift changes in EcDHFR-S148P or in MpDHFR. Contours are set so that DHFR·NADP^{+}·folate resonances appear open, to show areas of resonance overlap.

processed using NMRPipe[24] and analyzed using CcpNmr Analysis 2.2.2.[25]

Steady State Kinetic Measurements. Turnover rates were measured spectrophotometrically on a JASCO V-660 spectrophotometer by following the decrease in absorbance at 340 nm during the reaction (ε_{340} = 11800 M^{-1} cm^{-1}).[23] Initial rates were determined under saturating conditions (100 μM NADPH and DHF) at pH 7 in 100 mM potassium phosphate containing 100 mM NaCl and 10 mM β-mercaptoethanol and at pH 9 and 9.5 in MTEN buffer (50 mM MES, 25 mM Tris, 25 mM ethanolamine, 100 mM NaCl, and 10 mM β-mercaptoethanol). Temperature dependence measurements were performed in phosphate buffer because of the weak temperature dependence of its pK_a compared to that of organic amines. Product inhibition was assessed at pH 5 and 7 in MTEN buffer by measuring the initial rate with 100 nM enzyme, 100 μM NADPH, 100 μM DHF, and NADP^{+} concentrations of 0.5 μM, 5 μM, 50 μM, 500 μM, 5 mM, and 50 mM. The change in the initial rate with NADP^{+} concentration, normalized to the value without NADP^{+}, was fit to a sigmoidal curve using SigmaPlot 10. Michaelis constants were measured at pH 7 and 5 in MTEN buffer. To avoid hysteresis,[3] the enzyme (20−50 nM) was preincubated at the desired temperature with NADPH (0.1−200 μM) for 1 min prior to the addition of DHF (0.1−100 μM). When the concentration of NADPH was varied, that of DHF was maintained at 100 μM and *vice versa*. Each data point is the result of three independent measurements. The change in the initial rate with substrate concentration was fit to the Michaelis−Menten equation using SigmaPlot 10.

Pre-Steady State Kinetic Measurements. Hydride transfer rate constants were measured under single-turnover conditions on an Applied Photophysics stopped-flow spectrophotometer. The enzyme (final concentration of 20 μM) was preincubated with NADPH (final concentration of 8 μM) for at least 5 min in 100 mM potassium phosphate (pH 7.0) containing 100 mM NaCl and 10 mM β-mercaptoethanol, and the reaction was started by rapidly mixing with DHF (final concentration of 200 μM) in the same buffer. The loss of fluorescence resonance energy transfer from the enzyme to NADPH during the reaction was observed by exciting the sample at 292 nm and measuring the emission using an output filter with a 400 nm cutoff.

Dissociation Rate Constants. The rate constants of the release of product from the different binary and ternary complexes were measured using the competition method described previously.[3,26,27] The E·THF, E·NADP^{+}·THF, and E·NADPH·THF complexes were mixed with a large excess of MTX. The sample was excited at 292 nm, and the quenching of the fluorescence signal was monitored using a 305 nm cutoff filter.

dx.doi.org/10.1021/bi500507v | *Biochemistry* 2014, 53, 4761−4768

RESULTS AND DISCUSSION

Structure and Thermal Stability. Circular dichroism spectroscopy (Figures S4 and S5, Supporting Information) was used to demonstrate that EcDHFR-S148P and MpDHFR-P150S form folded proteins. The CD spectra were similar, but not identical, to those of the wild-type enzymes, consistent with some secondary structural differences in the apoenzyme conformational ensembles. MpDHFR-P150S was found to melt at 55.4 ± 0.2 °C, which is similar to the melting temperature of wild-type EcDHFR (51.6 ± 0.7 °C)[28] or wild-type MpDHFR in the presence of methotrexate (53.7 ± 0.6 °C) but considerably higher than that of MpDHFR (37.5 ± 0.8 °C).[9] The melting point of EcDHFR-S148P was 59.6 ± 0.2 °C, which is higher than that of wild-type EcDHFR. This shows that while the S148P mutation does not decrease the thermal stability of EcDHFR, MpDHFR is more tolerant of high temperatures after Pro150 is replaced with serine.

NMR spectroscopy was employed to investigate conformational changes following the chemical step of catalysis by the four DHFRs (Figure 2). As observed previously, a large difference is observed between the $^{1}H-^{15}N$ HSQC spectra of EcDHFR·NADP^{+}·folate and EcDHFR·NADP^{+}·THF (Figure 2A). Differences are seen throughout the enzyme but are largest in the M20, FG, and GH loops, consistent with a change from the closed to the occluded conformation.[14,29] In contrast, no substantial difference is observed between these two complexes for EcDHFR-S148P (Figure 2B), as seen previously for EcDHFR-S148A and EcDHFR-N23PP/S148A,[14] neither of which is capable of forming an occluded conformation. Similarly, no large difference is observed between the $^{1}H-^{15}N$ HSQC spectra of MpDHFR·NADP^{+}·folate and MpDHFR·NADP^{+}·THF (Figure 2C). This is consistent with our previous report of the NMR assignment of the MpDHFR·NADP^{+}·folate complex and comparison with other complexes.[30] Although some small changes were observed for residues surrounding the folate binding site and the cofactor pyrophosphate binding site, no significant changes were observed in the nicotinamide binding pocket or for the residues of the M20 and FG loops. These observations are consistent with there being no significant conformational change between the Michaelis complex and the product complex in MpDHFR.

In MpDHFR-P150S, which should be capable of forming the two hydrogen bonds necessary to stabilize the occluded conformation, the DHFR·NADP^{+}·THF complex gave lower-quality spectra compared to those of the DHFR·NADP^{+}·folate complex, and clear differences between the HSQC spectra of the two complexes were observed (Figure 2D). Several residues show resonance doubling, with the same resonance present as in the DHFR·NADP^{+}·folate complex plus a new resonance with a distinct chemical shift. As with the spectra for EcDHFR, the changes were seen throughout the protein but are most notable for G123 in the FG loop. The chemical shift perturbation for the additional resonance of G123V in MpDHFR-P150S is very similar to that of G121 in EcDHFR (Figure 2). We note that spectra of the product complex were acquired before those of the Michaelis complex mimic, and that both complexes were made up from a single preparation of the enzyme. In addition, one-dimensional ^{1}H NMR spectroscopy indicated no significant degradation of THF during the acquisition of the HSQC spectrum; the sample maintained its initial catalytic activity after acquisition of the HSQC spectrum, and the large excess of ligands coupled with the relative affinities of the four enzymes for NADP^{+} and THF (*vide infra*) makes incomplete binding of either ligand unlikely. It is also unlikely that MpDHFR-P150S becomes more dynamic on ligand binding, as it has been shown that apo-EcDHFR and apo-MpDHFR give HSQC spectra consistent with the presence of multiple conformations, whereas both enzymes show well-resolved HSQCs consistent with a single major conformation in a range of ligand complexes.[4,10,30,31] We are therefore confident that the lower quality of the spectra of the product complex indicates the presence of more than one species in solution rather than degradation, unfolding, or other loss of sample integrity. It is therefore likely that a proportion of MpDHFR-P150S is in an occluded-like conformation, in slow exchange with the closed conformation.

It has been shown that a number of bacterial DHFRs, including those with a proline residue at position 148 (EcDHFR numbering), give differences between the HSQC spectra of the DHFR·NADP^{+}·folate and DHFR·NADP^{+}·THF complexes greater than what would be expected simply from the replacement of folate.[32] In one such case, DHFR from *Staphylococcus aureus* (SaDHFR), a threonine residue is found at position 148 (Figure S3, Supporting Information), which is in principle capable of stabilizing an occluded conformation. At the time of writing, the PDB contains no crystal structures of SaDHFR in a complex expected to adopt the occluded conformation. While such clear differences in the HSQC spectra of the Michaelis and product complexes of these DHFRs[32] indicate that the hydride transfer step is accompanied by a conformational change, it is equally clear from our data that this change is not universally a transition between closed and occluded conformations.

Hydride Transfer. The pH dependence of the hydride transfer rate constant was measured under single-turnover conditions in MTEN buffer at 5 °C for MpDHFR and MpDHFR-P150S and at 25 °C for EcDHFR[18] and EcDHFR-S148P (Figure S6, Supporting Information). The two mutants were found to have similar pH dependencies with pK_a values around 6.5. The hydride transfer rate constants were similar to those of their wild-type counterparts (Supporting Information).

The kinetic isotope effect (KIE) on hydride transfer for MpDHFR-P150S and EcDHFR-S148P was found to depend on temperature in a fashion similar to that seen for MpDHFR and EcDHFR (Figure 3 and Supporting Information), indicating that altering either enzyme's ability to form the occluded conformation does not affect hydride transfer. Because both EcDHFR-S148A and MpDHFR can form the closed conformation,[8,14] this suggests that all DHFRs studied here are able to form the closed conformation, from which hydride transfer occurs, and further demonstrates that conformational changes between the closed and occluded conformations do not affect the actual chemistry of the reaction.

Steady State Kinetics. The pH dependence of the steady state rate constant k_{cat} for the MpDHFR-catalyzed reaction is bell-shaped with a maximum at pH ∼7 (Figure 4),[9] while that of EcDHFR is sigmoidal, as reported previously,[33] with a maximum at low pH (Figure 4). The decrease in k_{cat} for MpDHFR at low pH has been shown previously not to be due to protonation of His24 (the only ionic residue close to the active site) or enzyme inactivation.[9]

Interestingly, the pH dependence of k_{cat} for MpDHFR-P150S was found to be sigmoidal like that of EcDHFR, with a pH-independent k_{cat} of 14.5 ± 0.3 s^{-1}, very similar to the k_{cat} for wild-type MpDHFR at pH 7 and 20 °C (15.6 ± 0.2 s^{-1})[8] (Figure 4 and Supporting Information). On the other hand, a 5-fold decrease in

dx.doi.org/10.1021/bi500507v | *Biochemistry* 2014, 53, 4761−4768

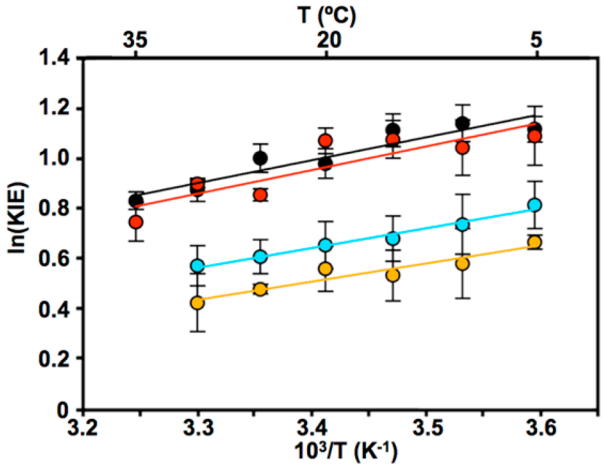

Figure 3. Kinetic isotope effect on hydride transfer at pH 7 by EcDHFR (black), EcDHFR-S148P (red), MpDHFR (cyan), and MpDHFR-P150S (orange), plotted on a logarithmic abscissa as a function of inverse temperature.

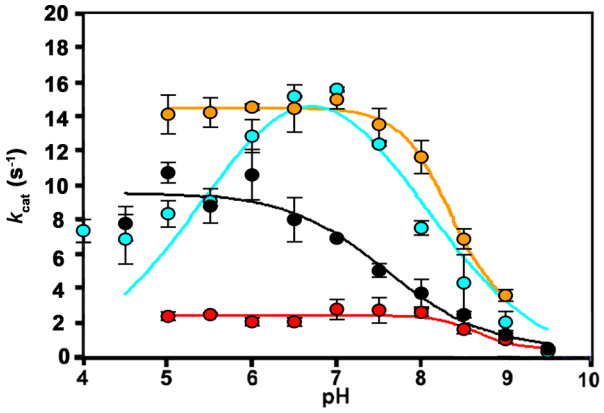

Figure 4. pH dependence of k_{cat} for MpDHFR[9] (cyan), MpDHFR-P150S (orange), EcDHFR (black), and EcDHFR-S148P (red) in MTEN buffer at 20 °C.

the value of k_{cat} was observed for EcDHFR-S148P ($2.1 \pm 0.2\ s^{-1}$) compared to that of wild-type EcDHFR ($10.6 \pm 1.5\ s^{-1}$) at pH 6 and 20 °C. Similar to their wild-type counterparts,[9,28] the two variants have a KIE of unity at pH ≤7 under steady state conditions (Supporting Information).

The Michaelis constants (K_M) for NADPH and DHF were measured for EcDHFR-S148P and MpDHFR-P150S at pH 7 and 5 at 20 °C (Table 1). Both variants have K_M values similar to those of their wild-type counterparts for both DHF and NADPH at pH 7, although the K_M for DHF with EcDHFR-S148P at pH 5 is 10 times higher than that of wild-type EcDHFR.

Table 1. K_M Values for NADPH and DHF with EcDHFR, EcDHFR-S148P, MpDHFR, and MpDHFR-P150S at 20 °C

enzyme	pH	K_M^{DHF} (μM)	K_M^{NADPH} (μM)
EcDHFR[a]	7	0.7 ± 0.2	4.8 ± 1.0
	5	0.7 ± 0.5	nd[d]
EcDHFR-S148P	7	0.7 ± 0.1	4.7 ± 0.7
	5	6.8 ± 0.5	5.5 ± 0.4
MpDHFR[b]	7.5	2.4 ± 0.2	5.7 ± 0.2
	5	0.4 ± 0.1[c]	10.8 ± 3.1
MpDHFR-P150S	7	2.2 ± 0.2	10.7 ± 0.6
	5	3.2 ± 0.5	15.2 ± 0.9

[a]Taken from ref 3. [b]Taken from ref 9. [c]At pH 5.5. [d]Not determined.

This type of bell-shaped steady state pH dependence has been seen previously when residues in helix αC (Figure 1A and Figure S3, Supporting Information) in EcDHFR were replaced by those of helix αC of LcDHFR.[34] A similar pH dependence was also obtained when a Glu-Lys-Asn three-residue stretch (as found in human DHFR) was inserted into the αC helix of EcDHFR.[35] While these two EcDHFR αC mutants have approximately the same k_H and k_{cat} as EcDHFR at pH 7, k_{cat} is reduced by 50% at lower pH,[34,35] similar to the case for MpDHFR.[9] In the case of the Glu-Lys-Asn insertion, the decrease in k_{cat} at low pH was demonstrated to be due to impaired dissociation of THF from the E·NADPH·THF complex,[35] which is the rate-limiting step in EcDHFR under steady state conditions.[3] However, this is not the case here, as the rate constant for dissociation of THF from MpDHFR·NADPH·THF is not affected by pH (*vide infra*).

Product Inhibition by $NADP^+$. The occluded conformation has been suggested to be important for avoiding product inhibition in EcDHFR.[2] It has been shown previously that EcDHFR-N23PP/S148A and human DHFR, neither of which can form the occluded conformation,[14] are more susceptible to product inhibition than wild-type EcDHFR.[32] This was indeed observed for EcDHFR-S148P, which gave an IC_{50} 22-fold lower than that observed for EcDHFR itself at pH 7 under our experimental conditions (Table 2 and Figure S7, Supporting Information). Similarly, MpDHFR is considerably more susceptible to product inhibition than EcDHFR, although less so than EcDHFR-S148P. MpDHFR-P150S is slightly less susceptible to product inhibition than wild-type MpDHFR, but more so than wild-type EcDHFR. This is consistent with its apparent ability to form more than one conformation in the product complex (*vide supra*), probably including an occluded-like conformation. Interestingly, the IC_{50} values for the four enzymes were all similar at pH 5, suggesting that the occluded conformation exerts no influence on $NADP^+$ affinity under acidic conditions.

Table 2. IC_{50} Values (micromolar) for $NADP^+$ with EcDHFR, EcDHFR-S148P, MpDHFR, and MpDHFR-P150S at 20 °C

enzyme	pH 5	pH 7
EcDHFR	159 ± 8	820 ± 59
EcDHFR-S148P	189 ± 9	40 ± 1
MpDHFR	317 ± 50	170 ± 11
MpDHFR-P150S	263 ± 29	321 ± 12

Dissociation Rate Constants for THF. The dissociation rate constants (k_{off}) for THF from different complexes (Table 3) were measured at pH 5−7 and 25 °C for MpDHFR and pH 6 and 25 °C for the two variants, to explore the rate-limiting step. Dissociation of THF from the MpDHFR·NADPH·THF mixed ternary complex is essentially unaffected by pH over the range measured (k_{off} values of 19.2 ± 2.3 at pH 7, 19.1 ± 2.0 at pH 6, and 15.7 ± 1.0 at pH 5). While the rate constant for this step is similar to the k_{cat} at pH 7, at higher pH hydride transfer becomes rate-limiting[9] and an alternative step must become rate-limiting at low pH. This cannot be a different product release step, as dissociation of THF from the MpDHFR·THF and MpDHFR·$NADP^+$·THF complexes is slower than k_{cat}, and so must presumably be the release of the oxidized cofactor or the subsequent rebinding of the reduced cofactor. The greater affinity of MpDHFR for DHF at low pH (at least as indicated by

dx.doi.org/10.1021/bi500507v | *Biochemistry* 2014, 53, 4761−4768

Table 3. Dissociation Rate Constants (k_{off}) for THF from the Various DHFRs, Measured Using the Competition Method with Methotrexate as the Trapping Ligand, at 25 °C in MTEN Buffer (pH 6)

	k_{off} (s^{-1})				
complex	EcDHFR[a]	MpDHFR	EcDHFR-S148P	MpDHFR-P150S	LcDHFR[b]
E·THF	0.97 ± 0.1	0.55 ± 0.1	0.5 ± 0.1	0.9 ± 0.2	0.5 ± 0.1
E·NADPH·THF	12.0 ± 1.0	19.1 ± 2.0	18.4 ± 0.8	17.3 ± 2.0	40.0 ± 8.0
E·$NADP^+$·THF	2.4 ± 0.3	3.8 ± 1.0	2.6 ± 0.1	2.5 ± 1.0	1.7 ± 0.2
k_{cat} (s^{-1})[c]	9.5 ± 1.4	15.4 ± 0.3	2.4 ± 0.3	14.5 ± 0.4	31.0 ± 2.0

[a]See ref 3. [b]See ref 26 (pH 6.5). [c]Maximal value (MpDHFR and LcDHFR) or pH-independent value (all others).

the K_M values) suggests, but cannot confirm, that DHF rebinding is not rate-limiting. The substantial kinetic isotope effect on hydride transfer measured by stopped-flow techniques[10] also supports this. An alternative possibility is that the catalytic cycle in MpDHFR becomes branched at low pH, with two distinct pathways contributing to the cycle, each with its own rate-determining step. Branching of the catalytic cycle has been suggested for other DHFRs,[36−39] for which the occluded conformation has not been observed and which lack the key serine residue for stabilizing this conformation.

For MpDHFR-P150S, the rate constant of release of THF at pH 6 from the E·NADPH·THF mixed ternary complex is also similar to the k_{cat} at pH 7. It is therefore likely that the k_{cat} for this variant is limited by dissociation of THF from the E·NADPH·THF complex at all pH values below 7, as is the case for EcDHFR.[3] In contrast, for EcDHFR-S148P, k_{cat} appears to be limited by the dissociation of THF from the E·$NADP^+$·THF product ternary complex, not from the E·NADPH·THF mixed ternary complex. This is different from the case for EcDHFR-N23PP/S148A; its $NADP^+$ affinity is sufficiently high that dissociation of this compound from the E·$NADP^+$ binary complex is the rate-limiting step.[14] All THF k_{off} values for EcDHFR-S148P and MpDHFR-P150S are similar to those of the wild-type enzymes, demonstrating that the mutations did not affect dissociation of THF.

Role of the Occluded Conformation. EcDHFR has often been used as a paradigmatic model system to study the role of protein motions for catalysis. Its catalytic cycle proceeds through a series of ordered steps with the release of THF from the E·NADPH·THF mixed ternary complex being rate-determining.[3] Moreover, EcDHFR was shown to oscillate between closed and occluded conformations,[2] and this has been proposed to aid progression through the catalytic cycle.[4,40−42] In EcDHFR, the closed to occluded conformational change must occur after the hydride transfer step, while it has been shown that the occluded to closed conformational change likely precedes the release of product from the mixed ternary complex.[43] This would indeed place a strong control on progression through the catalytic cycle and prevent product inhibition by reducing the affinity for $NADP^+$ relative to NADPH.

Previous work investigating the role of the occluded conformation has essentially focused on the effect of changes in the M20 loop. It has been shown that insertion of additional residues toward the C-terminal end of the M20 loop in vertebrate DHFRs compared to EcDHFR can account for the inability of vertebrate DHFRs to form the occluded conformation.[32] However, in MpDHFR, this region is highly similar to that of EcDHFR. Both have the same number of residues, and the differences, N23H and D27E substitutions (EcDHFR numbering), have been shown not to affect catalysis strongly.[9,44] Instead, conformational differences between bacterial DHFRs are likely to arise because of changes at position 148 (EcDHFR numbering). Differences earlier in the M20 loop, M16L and A19K substitutions, affect k_{cat} in EcDHFR but not MpDHFR and do not affect k_H in either (DOI: 10.1021/bi500508z). As k_{cat} reports on the release of THF from the DHFR·$NADP^+$·THF mixed ternary complex and the corresponding occluded-to-closed conformational change in EcDHFR, this provides further evidence of the involvement of M20 loop motions in progression through the catalytic cycle of EcDHFR but not that of MpDHFR.

EcDHFR-S148P is unable to form the occluded conformation and appears to bind $NADP^+$ more tightly than EcDHFR (likely slowing its release) without a significant change in its k_{off} for THF. This leads to a change in the rate-limiting step to the release of THF from the E·$NADP^+$·THF product ternary complex rather than from the E·NADPH·THF mixed ternary complex as is seen in EcDHFR. The rate constant for hydride transfer (k_H) and the Michaelis constants (K_M) remain essentially unaffected. Recent work in our group has shown that the chemistry in EcDHFR and MpDHFR is similar[10] and that conformational fluctuations in EcDHFR do not drive the chemical step of the reaction.[45−47]

MpDHFR similarly does not adopt the occluded conformation following the chemical step (*vide supra*), because of the presence of proline in place of the key residue, Ser148 in EcDHFR, that stabilizes this conformation. However, MpDHFR likely follows a well-ordered catalytic cycle similar to that of EcDHFR at pH 7. The release of product from the E·NADPH·THF mixed ternary complex is rate-limiting as is seen in EcDHFR, and the release of product from the E·$NADP^+$·THF complex clearly makes no significant contribution to the catalytic cycle despite the apparent elevated $NADP^+$ affinity compared to that of EcDHFR (Table 3). Furthermore, MpDHFR-P150S does show evidence supporting the formation of an occluded conformation and most likely follows a catalytic cycle similar to that of EcDHFR. The fact that this variant appears to have an affinity for $NADP^+$ lower than that of MpDHFR further indicates that the occluded conformation is important for $NADP^+$ release. The k_{cat} for MpDHFR shows a bell-shaped dependence on pH, instead of the sigmoidal curve observed for the EcDFHR reaction. The descending limb at low pH is removed when the occluded conformation is at least partially enabled in MpDHFR catalysis via the P150S mutation, although the complementary S148P mutation in EcDHFR does not cause the opposite effect and it is difficult to draw conclusions based on this observation.

Given its inability to form the occluded conformation, it is perhaps unclear how MpDHFR could faithfully follow the same catalytic cycle as EcDHFR. The k_{off} values for THF for the two enzymes are similar, as are the K_M values for NADPH, suggesting that MpDHFR does not simply have reduced affinity for both forms of the cofactor or slower THF release to compensate for the apparent increased $NADP^+$ affinity. MpDHFR also has a k_{off} for THF similar to that of LcDHFR (Table 3). Any effect must therefore be on $NADP^+$ release itself. Although the affinity of

MpDHFR for $NADP^+$ is greater than that of EcDHFR, it is not as great as for EcDHFR-S148P. This suggests that MpDHFR has additional features that reduce its affinity for $NADP^+$. A number of residues in the NADP(H) binding site are different between the two enzymes, which may influence the relative affinities of $NADP^+$ and NADPH. In addition, although two of the five steps of the EcDHFR catalytic cycle are accompanied by transitions between the closed and occluded conformations, the other three are not.[2] In these cases, progression through the catalytic cycle is driven by local changes to residue dynamics that promote ligand binding or release.[4] It is possible that such local dynamics are sufficient to control progression through all steps of the catalytic cycle in MpDHFR.

An alternative possibility is that *M. profunda* has a lower intracellular $NADP^+$ concentration, as seen in vertebrates. $NADP^+$ represents only 1% of the NADPH concentration in eukaryotic cells, but the two concentrations are equal in bacteria such as *E. coli*; it has been suggested that the fidelity of the order of steps in the catalytic cycle acts to prevent product inhibition in EcDHFR.[2] A lower $NADP^+$ concentration in *M. profunda* cells would similarly eliminate the need for MpDHFR to adopt strategies to avoid inhibition by this compound.

CONCLUSIONS

Here the role of the occluded conformation in DHFR catalysis was investigated by a combination of site-directed mutagenesis, steady state and pre-steady state kinetics, kinetic and equilibrium binding measurements, and NMR spectroscopy. The ability to adopt the occluded conformation does not affect hydride transfer proper. However, it is central to EcDHFR catalysis, because it controls this enzyme's affinity for $NADP^+$ and guides the enzyme through the steps of the catalytic cycle in a strictly ordered manner. Removal of the ability to form the occluded conformation has a great impact on EcDHFR, resulting in a change in the rate-limiting step and a decrease in the value of k_{cat}. In contrast, MpDHFR seems to follow a catalytic cycle similar to that of EcDHFR, but it functions efficiently without the involvement of an occluded conformation. Because many DHFRs lack a hydrogen bond donor in the position corresponding to Ser148 in EcDHFR, and because the occluded conformation has been observed only in EcDHFR, the occluded conformation is not a universal feature of bacterial DHFRs and the *E. coli* enzyme may therefore not always be the best choice for the study of general aspects of catalysis by dihydrofolate reductase.

ASSOCIATED CONTENT

Supporting Information

Circular dichroism spectra and melting profiles; steady state catalytic pathway for EcDHFR; additional figures demonstrating relevant structural features of DHFRs; product inhibition plots; tabulated data of the temperature dependence of k_H, k_{cat}, KIE(k_H), and KIE(k_{cat}) at pH 7; temperature dependencies of k_{cat} and KIE at pH 9 and 9.5; steady state and pre-steady state activation energies and Arrhenius prefactors; and pH dependence of k_H, k_{cat}, KIE(k_H), and KIE(k_{cat}). This material is available free of charge via the Internet at http://pubs.acs.org.

AUTHOR INFORMATION

Corresponding Authors

*School of Chemistry, Cardiff University, Main Building, Park Place, Cardiff CF10 3AT, United Kingdom. E-mail: loveridgeej@cf.ac.uk. Phone: (44) 29 2087 4029.

*E-mail: allemannrk@cf.ac.uk. Phone: (44) 29 2087 9014.

Author Contributions

E.M.B. performed the bulk of the experimental work. L.Y.P.L., S.M.M., and E.J.L. performed additional experimental work. E.M.B., E.J.L., and R.K.A. designed the experiments and wrote the manuscript.

Funding

This work was supported by Grants BB/E008380/1 and BB/J005266/1 (R.K.A.) from the UK Biotechnology and Biological Sciences Research Council and by Cardiff University.

Notes

The authors declare no competing financial interests.

ABBREVIATIONS

DHFR, dihydrofolate reductase; EcDHFR, DHFR from *E. coli*; MpDHFR, DHFR from *M. profunda*; BaDHFR, DHFR from *B. anthracis*; LcDHFR, DHFR from *L. casei*; SaDHFR, DHFR from *S. aureus*; $NADP^+$, nicotinamide adenine dinucleotide phosphate; NADPH, nicotinamide adenine dinucleotide phosphate (reduced form); DHF, dihydrofolate; THF, tetrahydrofolate; MTX, methotrexate; DDF, 5,10-dideazatetrahydrofolate; KIE, kinetic isotope effect; pABG, *p*-aminobenzoyl-L-glutamate; PDB, Protein Data Bank.

REFERENCES

(1) Blakley, R. L. (1984) in *Folates and Pterins* (Blakley, R. L., and Benkovic, S. J., Eds.) pp 191−253, Wiley, New York.

(2) Sawaya, M. R., and Kraut, J. (1997) Loop and subdomain movements in the mechanism of *Escherichia coli* dihydrofolate reductase: Crystallographic evidence. *Biochemistry 36*, 586−603.

(3) Fierke, C. A., Johnson, K. A., and Benkovic, S. J. (1987) Construction and Evaluation of the Kinetic Scheme Associated with Dihydrofolate Reductase from *Escherichia coli*. *Biochemistry 26*, 4085−4092.

(4) Boehr, D. D., McElheny, D., Dyson, H. J., and Wright, P. E. (2006) The dynamic energy landscape of dihydrofolate reductase catalysis. *Science 313*, 1638−1642.

(5) Xu, Y., Nogi, Y., Kato, C., Liang, Z. Y., Ruger, H. J., De Kegel, D., and Glansdorff, N. (2003) *Moritella profunda sp nov.* and *Moritella abyssi sp nov.*, two psychropiezophilic organisms isolated from deep Atlantic sediments. *Int. J. Syst. Evol. Microbiol. 53*, 533−538.

(6) Xu, Y., Feller, G., Gerday, C., and Glansdorff, N. (2003) *Moritella* cold-active dihydrofolate reductase: Are there natural limits to optimization of catalytic efficiency at low temperature? *J. Bacteriol. 185*, 5519−5526.

(7) Hata, K., Kono, R., Fujisawa, M., Kitahara, R., Kamatari, Y. O., Akaska, K., and Xu, Y. (2004) High pressure NMR study of dihydrofolate reductase from a deep-sea bacterium *Moritella profunda*. *Cell. Mol. Biol. (Oxford) 50*, 311−316.

(8) Hay, S., Evans, R. M., Levy, C., Loveridge, E. J., Wang, X., Leys, D., Allemann, R. K., and Scrutton, N. S. (2009) Are the Catalytic Properties of Enzymes from Piezophilic Organisms Pressure Adapted? *ChemBioChem 10*, 2348−2353.

(9) Evans, R. M., Behiry, E. M., Tey, L. H., Guo, J. N., Loveridge, E. J., and Allemann, R. K. (2010) Catalysis by Dihydrofolate Reductase from the Psychropiezophile *Moritella profunda*. *ChemBioChem 11*, 2010−2017.

(10) Loveridge, E. J., Tey, L.-H., Behiry, E. M., Dawson, W. M., Evans, R. M., Whittaker, S. B.-M., Guenther, U. L., Williams, C., Crump, M. P., and Allemann, R. K. (2011) The Role of Large-Scale Motions in Catalysis by Dihydrofolate Reductase. *J. Am. Chem. Soc. 133*, 20561−20570.

(11) Gargaro, A. R., Soteriou, A., Frenkiel, T. A., Bauer, C. J., Birdsall, B., Polshakov, V. I., Barsukov, I. L., Roberts, G. C. K., and Feeney, J. (1998) The solution structure of the complex of *Lactobacillus casei* dihydrofolate reductase with methotrexate. *J. Mol. Biol. 277*, 119−134.

(12) Feeney, J., Birdsall, B., Kovalevskaya, N. V., Smurnyy, Y. D., Navarro Peran, E. M., and Polshakov, V. I. (2011) NMR Structures of Apo *L. casei* Dihydrofolate Reductase and Its Complexes with Trimethoprim and NADPH: Contributions to Positive Cooperative Binding from Ligand-Induced Refolding, Conformational Changes, and Interligand Hydrophobic Interactions. *Biochemistry 50*, 3609−3620.
(13) Beierlein, J. M., Frey, K. M., Bolstad, D. B., Pelphrey, P. M., Joska, T. M., Smith, A. E., Priestley, N. D., Wright, D. L., and Anderson, A. C. (2008) Synthetic and Crystallographic Studies of a New Inhibitor Series Targeting *Bacillus anthracis* Dihydrofolate Reductase. *J. Med. Chem. 51*, 7532−7540.
(14) Bhabha, G., Lee, J., Ekiert, D. C., Gam, J., Wilson, I. A., Dyson, H. J., Benkovic, S. J., and Wright, P. E. (2011) A dynamic knockout reveals that conformational fluctuations influence the chemical step of enzyme catalysis. *Science 332*, 234−238.
(15) Benkovic, S. J., Fierke, C. A., and Naylor, A. M. (1988) Insights into Enzyme Function from Studies on Mutants of Dihydrofolate Reductase. *Science 239*, 1105−1110.
(16) Blakley, R. L. (1960) Crystalline dihydropteroylglutamic acid. *Nature 188*, 231−232.
(17) Mathews, C. K., and Huennekens, F. M. (1960) Enzymic Preparation of the L,L-Diastereoisomer of Tetrahydrofolic Acid. *J. Biol. Chem. 235*, 3304−3308.
(18) Loveridge, E. J., and Allemann, R. K. (2011) Effect of pH on Hydride Transfer by *Escherichia coli* Dihydrofolate Reductase. *ChemBioChem 12*, 1258−1262.
(19) Swanwick, R. S., Maglia, G., Tey, L., and Allemann, R. K. (2006) Coupling of protein motions and hydrogen transfer during catalysis by *Escherichia coli* dihydrofolate reductase. *Biochem. J. 394*, 259−265.
(20) Wang, X.-T., Chan, T. F., Lam, V. M. S., and Engel, P. C. (2008) What is the role of the second "structural" $NADP^+$-binding site in human glucose 6-phosphate dehydrogenase? *Protein Sci. 17*, 1403−1411.
(21) Seeger, D. R., Cosulich, D. B., Smith, J. M., and Hultquist, M. E. (1949) Analogs of Pteroylglutamic Acid. III. 4-Amino Derivatives. *J. Am. Chem. Soc. 71*, 1753−1758.
(22) Zakrzewski, S. F., and Sansone, A. M. (1971) A new synthesis of tetrahydrofolic acid. *Methods Enzymol. 18*, 728−731.
(23) Stone, S. R., and Morrison, J. F. (1982) Kinetic mechanism of the reaction catalyzed by dihydrofolate reductase from *Escherichia coli*. *Biochemistry 21*, 3757−3765.
(24) Delaglio, F., Grzesiek, S., Vuister, G. W., Zhu, G., Pfeifer, J., and Bax, A. (1995) Nmrpipe: A Multidimensional Spectral Processing System Based on Unix Pipes. *J. Biomol. NMR 6*, 277−293.
(25) Vranken, W. F., Boucher, W., Stevens, T. J., Fogh, R. H., Pajon, A., Llinas, M., Ulrich, E. L., Markley, J. L., Ionides, J., and Laue, E. D. (2005) The CCPN data model for NMR spectroscopy: Development of a software pipeline. *Proteins 59*, 687−696.
(26) Birdsall, B., Burgen, A. S. V., and Roberts, G. C. K. (1980) Binding of coenzyme analogs to *Lactobacillus casei* dihydrofolate reductase: Binary and ternary complexes. *Biochemistry 19*, 3723−3731.
(27) Andrews, J., Fierke, C. A., Birdsall, B., Ostler, G., Feeney, J., Roberts, G. C. K., and Benkovic, S. J. (1989) A Kinetic Study of Wild-Type and Mutant Dihydrofolate Reductases from *Lactobacillus casei*. *Biochemistry 28*, 5743−5750.
(28) Swanwick, R. S., Shrimpton, P. J., and Allemann, R. K. (2004) Pivotal role of Gly 121 in dihydrofolate reductase from *Escherichia coli*: The altered structure of a mutant enzyme may form the basis of its diminished catalytic performance. *Biochemistry 43*, 4119−4127.
(29) Venkitakrishnan, R. P., Zaborowski, E., McElheny, D., Benkovic, S. J., Dyson, H. J., and Wright, P. E. (2004) Conformational changes in the active site loops of dihydrofolate reductase during the catalytic cycle. *Biochemistry 43*, 16046−16055.
(30) Loveridge, E. J., Matthews, S. M., Williams, C., Whittaker, S. B.-M., Günther, U. L., Evans, R. M., Dawson, W. M., Crump, M. P., and Allemann, R. K. (2013) Aliphatic ^1H, ^{13}C and ^{15}N chemical shift assignments of dihydrofolate reductase from the psychropiezophile *Moritella profunda* in complex with $NADP^+$ and folate. *Biomol. NMR Assignments 7*, 61−64.
(31) Osborne, M. J., Schnell, J., Benkovic, S. J., Dyson, H. J., and Wright, P. E. (2001) Backbone dynamics in dihydrofolate reductase complexes: Role of loop flexibility in the catalytic mechanism. *Biochemistry 40*, 9846−9859.
(32) Bhabha, G., Ekiert, D. C., Jennewein, M., Zmasek, C. M., Tuttle, L. M., Kroon, G., Dyson, H. J., Godzik, A., Wilson, I. A., and Wright, P. E. (2013) Divergent evolution of protein conformational dynamics in dihydrofolate reductase. *Nat. Struct. Mol. Biol. 20*, 1243−1249.
(33) Stone, S. R., and Morrison, J. F. (1984) Catalytic mechanism of the dihydrofolate reductase reaction as determined by pH studies. *Biochemistry 23*, 2753−2758.
(34) Li, L., and Benkovic, S. J. (1991) Impact on catalysis of secondary structural manipulation of the αC-helix of *Escherichia coli* dihydrofolate reductase. *Biochemistry 30*, 1470−1478.
(35) Posner, B. A., Li, L. Y., Bethell, R., Tsuji, T., and Benkovic, S. J. (1996) Engineering specificity for folate into dihydrofolate reductase from *Escherichia coli*. *Biochemistry 35*, 1653−1663.
(36) Davies, J. F., Delcamp, T. J., Prendergast, N. J., Ashford, V. A., Freisheim, J. H., and Kraut, J. (1990) Crystal Structures of Recombinant Human Dihydrofolate Reductase Complexed with Folate and 5-Deazafolate. *Biochemistry 29*, 9467−9479.
(37) Kovalevskaya, N., Smurnyy, Y., Polshakov, V., Birdsall, B., Bradbury, A., Frenkiel, T., and Feeney, J. (2005) Solution Structure of Human Dihydrofolate Reductase in its Complex with Trimethoprim and NADPH. *J. Biomol. NMR 33*, 69−72.
(38) Czekster, C. M., Vandemeulebroucke, A., and Blanchard, J. S. (2011) Two Parallel Pathways in the Kinetic Sequence of the Dihydrofolate Reductase from *Mycobacterium tuberculosis*. *Biochemistry 50*, 7045−7056.
(39) Appleman, J. R., Beard, W. A., Delcamp, T. J., Prendergast, N. J., Freisheim, J. H., and Blakley, R. L. (1990) Unusual transient- and steady-state kinetic behavior is predicted by the kinetic scheme operational for recombinant human dihydrofolate reductase. *J. Biol. Chem. 265*, 2740−2748.
(40) Miller, G. P., and Benkovic, S. J. (1998) Deletion of a highly motional residue affects formation of the Michaelis complex for *Escherichia coli* dihydrofolate reductase. *Biochemistry 37*, 6327−6335.
(41) Miller, G. P., Wahnon, D. C., and Benkovic, S. J. (2001) Interloop contacts modulate ligand cycling during catalysis by *Escherichia coli* dihydrofolate reductase. *Biochemistry 40*, 867−875.
(42) McElheny, D., Schnell, J. R., Lansing, J. C., Dyson, H. J., and Wright, P. E. (2005) Defining the role of active-site loop fluctuations in dihydrofolate reductase catalysis. *Proc. Natl. Acad. Sci. U.S.A. 102*, 5032−5037.
(43) Weikl, T. R., and Boehr, D. D. (2012) Conformational selection and induced changes along the catalytic cycle of *Escherichia coli* dihydrofolate reductase. *Proteins 80*, 2369−2383.
(44) Loveridge, E. J., Dawson, W. M., Evans, R. M., Sobolewska, A., and Allemann, R. K. (2011) Reduced Susceptibility of *Moritella profunda* Dihydrofolate Reductase to Trimethoprim is Not Due to Glutamate 28. *Protein J. 30*, 546−548.
(45) Loveridge, E. J., Behiry, E. M., Guo, J., and Allemann, R. K. (2012) Evidence that a 'dynamic knockout' in *Escherichia coli* dihydrofolate reductase does not affect the chemical step of catalysis. *Nat. Chem. 4*, 292−297.
(46) Luk, L. Y. P., Ruiz-Pernia, J. J., Dawson, W. M., Roca, M., Loveridge, E. J., Glowacki, D. R., Harvey, J. N., Mulholland, A. J., Tuñón, I., Moliner, V., and Allemann, R. K. (2013) Unraveling the role of protein dynamics in dihydrofolate reductase catalysis. *Proc. Natl. Acad. Sci. U.S.A. 110*, 16344−16349.
(47) Ruiz-Pernia, J. J., Luk, L. Y. P., García-Meseguer, R., Martí, S., Loveridge, E. J., Tuñón, I., Moliner, V., and Allemann, R. K. (2013) Increased Dynamic Effects in a Catalytically Compromised Variant of *Escherichia coli* Dihydrofolate Reductase. *J. Am. Chem. Soc. 135*, 18689−18696.